ELSEVIER

Journal of Chromatography B, 699 (1997) 29–45

JOURNAL OF CHROMATOGRAPHY B

Review

Protein separation using non-porous sorbents

Wen-Chien Lee

Department of Chemical Engineering, National Chung Cheng University, Chiayi 621, Taiwan

Abstract

This article overviews the development of non-porous sorbents having small particle diameters which have proven effective for rapid analysis and micropreparative separation of proteins by liquid chromatography. Much attention is given to the preparation and application of silica- and polystyrene-based non-porous packings for various chromatographic modes, especially affinity chromatography. Modeling works on the prediction and parameter estimation for the dynamics of protein adsorption using non-porous sorbents are reviewed and briefly described. To conclude this review, future prospects of the application of non-porous sorbents are also presented. © 1997 Elsevier Science B.V.

Keywords: Reviews; Proteins

Contents

1. Introduction

Non-porous sorbents of microsize have been gaining great interest since the mid 1980s for the rapid high-performance liquid chromatography (HPLC) of proteins. The typical structure of non-porous stationary phase is a fluid-impervious support which is covered (physically or covalently attached) with a layer of functional groups on its surface. A non-porous sorbent with a fluid-impervious core is also called micropellicular stationary phase [1]. In 1967, Horvath et al. named the surface-functionally coated particle as the pellicular stationary phase [2]. They roughened the surface of the glass beads (30–40 μm in diameter) and covered it with a film of styrene–divinylbenzene polymer that was later sulfonated.

0378-4347/97/$17.00 Copyright © 1997 Elsevier Science B.V. All rights reserved
PII S0378-4347(97)00179-5

Diffusion effects due to the pore structure could be eliminated; however, the capacity was very low due to the small surface area of the non-porous particles. In the eighties, the particle size was decreased to 1.5–7 μm in order to increase the loading capacity. A major advantage of the non-porous sorbents is that significant intraparticle diffusion resistances are absent; this is particularly useful for the rapid analysis of proteins with high efficiency and resolution [3]. The rapid separation makes it very useful for quality control, on-line monitoring, and purity check of biomolecules, such as peptide mapping of recombinant products [4]. Non-porous packings are also ideal for studying the fundamental retention mechanism of both proteins and low-molecular-mass solutes, since both the kinetic and thermodynamic properties of the interactions between the solute in the mobile phase and the ligand in the stationary phase can be studied separate from the effects of the porous structure [5]. The potential of using non-porous sorbents, for example, for the study of the conformational change of proteins adsorbed on chromatographic supports has been elucidated [6].

At the same time, the lack of internal pore structure offers certain other advantages, such as good recovery of mass and biological activity in protein chromatography. When used for micro-preparative separation of active molecules, the loss of activity due to diffusion through the pores can be eliminated. Although the loading capacity of columns packed with non-porous sorbents is relative low for small molecules, it is not much smaller than the capacity of totally porous sorbents for macromolecules such as proteins [7]. Experimental capacities of the non-porous sorbents were found to be comparable to those of porous silica-dye affinity sorbents and higher than that of larger glass beads (5–40 μm) as determined by frontal analysis experiments [8].

In the present article, the use of non-porous sorbents for protein chromatography is reviewed. It is found that commercialized prepacked columns are currently available for ion-exchange, reversed-phase and hydrophobic interaction chromatography of proteins (Table 1). Thus, much attention will be given to the preparation and application of affinity sorbents derived from non-porous particles. In addition to experimental studies, modeling works on the prediction of the dynamics of protein adsorption provide an excellent basis for the design and optimization of a liquid chromatographic process with non-porous sorbents operated in either analytical or preparative mode. The development of a mathematical model describing the dynamics of protein adsorption in

Table 1
Commercially available pre-packed columns with non-porous sorbents

Column trademark	Column size	Packing material	Functional group	Manufacturer	Application[a]	References
HYTACH C18	30×4.6 mm I.D.	2 μm, silica	C_{18}	Glycotech (Hamden, CT, USA)	RP	O'Keefe and Paiva [17]
MICRA NPS RP-18	53×4.6 mm I.D.	1.5 μm silica	C_{18}	Micra Scientific (Northbrook, USA)	RP	Rudolphi et al. [18]
Develosil NP ODS-2	10×4.0 mm I.D.	2 μm silica	C_{18}	Nomura (Seto City, Japan)	RP	Company's catalog
NP ODS-5	30×4.0 mm I.D.	5 μm silica	C_{18}		RP	
Hydrocell DEAE NP10	35×4.6 mm I.D. or other sizes	10 μm PS-DVB	diethylaminoethyl	BioChrom Labs, Inc., (Terre Haute, USA)	AE	Company's catalog
QA NP10	35×4.6 mm I.D. or other sizes	10 μm PS-DVB	diethylmethylaminoethyl		AE	
SP NP10	35×4.6 mm I.D. or other sizes	10 μm PS-DVB	sulfopropyl		CE	
C3 NP10	35×4.6 mm I.D. or other sizes	10 μm PS-DVB	allyl		HIC	
C4 NP10	35×4.6 mm I.D. or other sizes	10 μm PS-DVB	butyl		HIC	
Hamilton PRP-∞	30×4.1 mm I.D.	4 μm PS-DVB		Hamilton Co. (Reno, USA)	RP	Pastores et al. [50]
Bio-Gel MA7P	30×4.6 mm I.D.50×7.8 mm I.D.	7 μm polymethacrylate	PEI	Bio-Rad Labs. (Hercules, USA)	AE	Company's catalog
MA7C	30×4.6 mm I.D.50×7.8 mm I.D.		Carboxyl		CE	
MA7S	50×7.8 mm I.D.		Sulfopropyl		CE	
MA7Q	50×7.8 mm I.D.		Quaternary amine		AE	
TSK Butyl-NPR	35×4.6 mm I.D.	2.5 μm polymer	butyl	Tosoh Corp. (Tokyo, Japan)	HIC	Company's catalog
TSK SP-NPR	35×4.6 mm I.D.	2.5 μm	sulphopropyl		CE	
TSK DEAE-NPR	35×4.6 mm I.D.	2.5 μm	diethylaminoethyl		AE	
TSK Octadecyl-NPR	35×4.6 mm I.D.	2.5 μm	octadecyl		RP	

[a] Application modes: RP, reversed-phase; AE, anion-exchange; CE, Cation-exchange; HIC, hydrophobic interaction chromatography.

columns packed with affinity and ion-exchange sorbents will thus be reviewed and discussed.

2. Protein chromatography using non-porous sorbents

Silica-based sorbents are the most widely used for packings of HPLC columns due to their high mechanical strength that can resist a large back pressure when operated at a high flow-rate. Starting from 1984, laboratory-made non-porous silica particles of diameter 1.5 μm were prepared and bonded with *n*-octadecyl and *n*-octyl groups for the separation of proteins and peptides [9–11]. Short columns (35×8 mm I.D.) packed with these non-porous reversed-phase materials are effective for mixtures of proteins and mixtures of small peptides. When the reversed-phase columns are operated in gradient elution, losses of the biological activity of the proteins often occur. However, after the 1.5 μm silica particles are converted to amide- and ether-bound silica for the separation of proteins, fast separation (in less than 5 min) can be achieved with high biological recoveries [12]. Non-porous silica with a slightly larger diameter (2.0 μm) was also prepared in Horvath's laboratory and derived with octadecyl groups for the rapid analysis of proteins and peptides. A mixture of five proteins (25–50 ng each) were separated on a 30× 4.6 mm I.D. column in 20 s at a flow-rate of 4 ml/min [13,14]. Non-porous silica particles having mean diameters of 2, 5 and 20 μm (manufactured by Nomura, Seto, Japan) were chemically modified with *n*-octadecyldimethylchlorosilane and respectively packed in columns for the purification of proteins [15,16]. Nimura et al. [15] found that the efficiencies of these reversed-phase columns were approximately the same for all particle sizes. Other commercialized prepacked reversed-phase columns with non-porous silica-based sorbents (see Table 1) include the HYTACH C_{18} column that has been tested for analysis of recombinant hepatitis B surface antigen [17] and the MICRA NPS RP-18 column for analysis of urinary catecholamines [18]. Anion-exchangers for protein adsorption were made by Janzen et al. [19] with PEI bonded to the non-porous silica using a procedure introduced by Chang et al. [20]. Hearn and Unger's groups also modified non-porous silica (with a particle diameter 1.5 or 2.1 μm) with different silanes for the immobilization of affinity ligands including antibody and triazine dyes such as Cibacron Blue F3GA [8,21–23]. The laboratory-made non-porous silica was also modified with γ-aminopropyltriethoxysilane and coupled with protein A for rapid analysis of human IgG [24]. Non-porous, fused-silica microspheres (2 μm) obtained from Glycotech (Hamden, CT, USA) were epoxylated and coupled with iminodiacetic acid at the surface for rapid analysis of proteins by metal-interaction chromatography [25].

In 1986, Burke et al. [26,27] in Bio-Rad Labs. used spherical non-porous polymethacrylate beads with polyethyleneimine (PEI) covalently coupled to the surface for rapid resolution of proteins. A mixture containing five proteins can be separated with a 30×4.6 mm I.D. column in 90 s with a flow-rate of 4.5 ml/min. Protein recoveries for a loading of 100 μg are greater than 89%. The trademark of a Bio-Rad column, Microanalyzer MA7P, was lately changed to Bio-Gel MA7P. The performance of the non-porous packings was compared with a number of similar porous HPLC packings. Duncan et al. found that the non-porous columns were equally efficient for proteins spanning a wide range of molecular masses, while the porous columns exhibited decreasing efficiency as the proteins become larger [28]. The column packed with non-porous PEI-coated polymethacrylate beads was converted to a strong anion-exchange column for proteins by in situ quaternization [29]. Other non-porous polymer-based packings for the separation of proteins and other biopolymers are the TSK gel NPR series: DEAE-NPR, SP-NPR, Octadecyl-NPR and Butyl-NPR. They are prepared by chemically bonding diethylaminoethyl, sulphopropyl, octadecyl and butyl groups onto the surface of non-porous synthetical polymer beads of particle diameter 2.5 μm. The exact chemical composition of the base material is not stated by the manufacturer, yet it seems to be a methacrylate-based polymer according to Rounds and Regnier [30]. According to Hashimoto [31], it contains many primary hydroxyl groups and the ligands described above are introduced by utilizing the hydroxyl groups. All types of TSK gel are packed in 35×4.6 mm I.D. columns. Kato et al. used the DEAE-NPR column for the separation of a four-

protein mixture (conalbumin, transferrin, ovalbumin and trypsin inhibitor) in 5 min at a flow-rate of 1.5 ml/min and the SP-NPR column for a five-protein mixture (trypsinogen, α-chymotrypsinogen A, ribonuclease A, cytochrome *c* and lysozyme) in 6 min at the same flow-rate [32]. Recovery of proteins (5 μg each) from the DEAE-NPR column is greater than 91%. The DEAD-NPR column was also effective for separation of phosphorylated calmodulin from non-phosphorylated calmodulin [33]. SP-NPR was also effective for the separation of glycated hemoglobin A_{1C} from other hemoglobin variants in less than 10 min [34]. High-performance hydrophobic interaction chromatography of proteins on the Butyl-NPR was examined by Kato et al. [35]. The loading capacity of proteins, however, was fairly low (1–2 μg for pure samples) in compared with the above-mentioned ion-exchange columns (around 5 μg). This Butyl-NPR column was recently employed operating in a displacement mode for the separation of a mixture of ribonuclease and lysozyme using BSA as the displacer in a carrier containing 2.3 *M* ammonia sulfate [36]. TSK octadecyl-NPR was employed in reversed-phase HPLC of proteins and peptides [4,37]. A six-protein mixture containing 50 ng of each protein can be separated in 6 min. For 400 ng loads, the recovery of proteins is much higher, greater than 94% for all tested proteins [4]. This reversed-phase resin was also employed for monitoring the production of recombinant human granulocyte colony stimulating factor produced in *E. coil* cells [38].

A highly crosslinked copolymer of styrene and divinylbenzene (PS–DVB) microspheres having a rugulose surface and a mean diameter of 3 μm was prepared by suspension polymerization and packed into a 30×4.6 mm I.D. column for reversed-phase HPLC of proteins and peptides [3]. On this column, a mixture of six proteins (460 ng totally) can be chromatographically analyzed at room temperature in about 40 s at an eluent flow-rate of 3 ml/min. Rounds and Regnier [30] prepared a strong anion-exchanger with 3 μm non-porous PS–DVB particles by adsorbance coating with PEI. A mixture of four proteins can be separated in 60 s on a column (5×6 mm I.D.) packed with the PEI coated sorbents at a flow-rate of 3 ml/min. Anion-exchangers also were prepared from non-porous, 4 or 4.5 μm PS–DVB beads (with 10% crosslinking) by coating with different anion-exchange latexes [39–41]. According to Varga et al. [42], the polystyrene-based resins are promising for surface modification and immobilization of ligands for high-performance affinity chromatography (HPAC) of proteins. A 2.5 μm PS–DVB bead was surface coated with dinitrophenyl amino acid, using carbodiimide as catalyst, for affinity chromatography of immunoglobulin E [43]. Polystyrene (PS) microbeads (4 μm in diameter) were prepared, coated with poly(vinyl alcohol) by adsorption and chemical crosslinking, and then Cibacron Blue F3GA was attached for adsorption of specific albumin [44]. A procedure for surface modification and ligand immobilization on microsized non-porous PS was recently reported [45]. PS was converted to aromatic amino-containing PS by nitration and successive reduction (hydrogenation). Two affinity ligands, *p*-aminophenyl-β-D-glcopyranoside and *p*-aminobenzamidine, were covalently coupled to this amino-containing PS and the columns packed with the resulting affinity sorbents were effective for quantitative analysis of concanavalin A (Con A) and trypsin, respectively. In preparing the sorbents for reversed-phase HPLC of proteins and oligonucleotides, 2.1 μm non-porous PS–DVB was alkylated under Friedel–Crafts conditions to introduce C_{18} groups [46–48]. A column packed with the non-porous reversed-phase sorbents was commercialized by CETAC Technologies (Omaha, NE, USA). A mixture of seven proteins was separated in 45 s at a flow-rate of 4.5 ml/min at 80°C [49]. The polystyrene-based polymer can be used directly as an adsorbent for reversed-phase chromatography. The column PRP-Infinity (30×4.1 mm I.D.) packed with non-porous PS–DVB beads was made by Hamilton and used for HPLC of porcine insulin [50]. HPLC using non-porous sorbents proved very useful in the case of separating a larger protein from a complex mixture of low-molecular-mass compounds with different physicochemical properties. Recently, laboratory-made polystyrene-based 3 μm non-porous particles with a covalently attached hydrophilic layer containing butyl moieties at the surface were employed for hydrophobic interaction of proteins operated in the displacement mode [35].

Non-porous sorbents other than silica- and syn-

thetic polymer-based packings were obtained from crosslinked 12% agarose beads. Hjerten and Liao described a procedure of converting macroporous agarose beads into non-porous beads (about 20 μm) by shrinkage and crosslinking in organic solvents [51]. Columns packed with the compressed, non-porous agarose beads were used for hydrophobic interaction chromatography of proteins [51,52]. These beads derivatized with ion-exchanging groups and affinity ligand (human growth hormone) were packed into columns for the ion-exchange [53,54] and immuno-affinity chromatography [55] of proteins, respectively. Other special types of pellicular sorbents for protein separation include non-porous glass beads, glass-coated PS beads and zirconia-based particles. McCoy et al. described the immobilization of anti-β-galactosidase ligand on the non-porous glass-coated beads having a mean diameter of 172 μm and a polystyrene-based core, and used those for the adsorption of β-galactosidase [56]. The development of zirconia-based sorbents is recently of interest because of their higher stability at alkaline pH. The synthesis of non-porous microspherical octadecyl-zirconia particles was described by Yu and El Rassi [57].

3. Preparation and application of silica-based non-porous sorbents

Non-porous silica particles having a diameter ranging from less than 0.05 μm to 2 μm are usually synthesized via the hydrolysis of tetraalkyl orthosilicates and the subsequent condensation of silicic acid in alcoholic solution as described in the paper of Stober et al. [58]. The growth of silica beads was controlled by the concentration of ammonia, the composition of the alcohol solution, the kind of tetraakyl orthosilicate used and the reaction time. The use of tetraamyl orthosilicate under constant experimental conditions causes a larger particle size than that with tetraethyl orthosilicate. The higher the concentration of ammonia employed, the larger the mean particle size. The recipes as described elsewhere produced non-porous silica particles with an average diameter of 1.4 μm and a specific surface area of 5.2 m^2/g [24]. The particle size distribution of the prepared silica determined by using Electrophoresis Cell AZ4 (Malvern Instruments) is shown in Fig. 1. The specific surface area was determined with an ASAP 2000 instrument (Micromeritics Instruments) and calculated with the BET equation using nitrogen as the adsorbate. A comparison of experimental and theoretical surface areas of the silicas in various particle diameters is shown in Fig. 2.

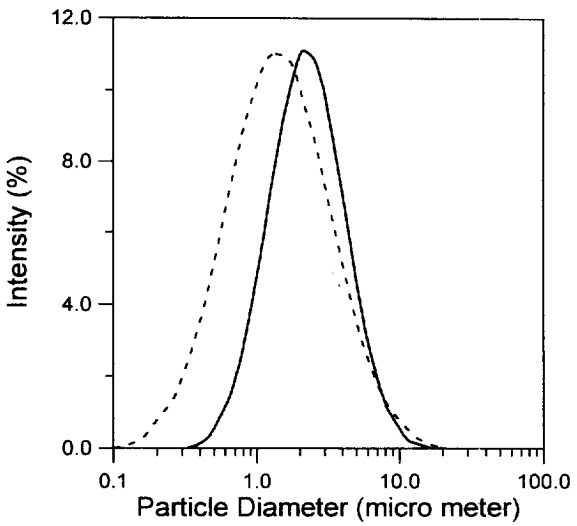

Fig. 1. Particle size distribution of the prepared non-porous silica (dashed line) and polystyrene beads (solid line).

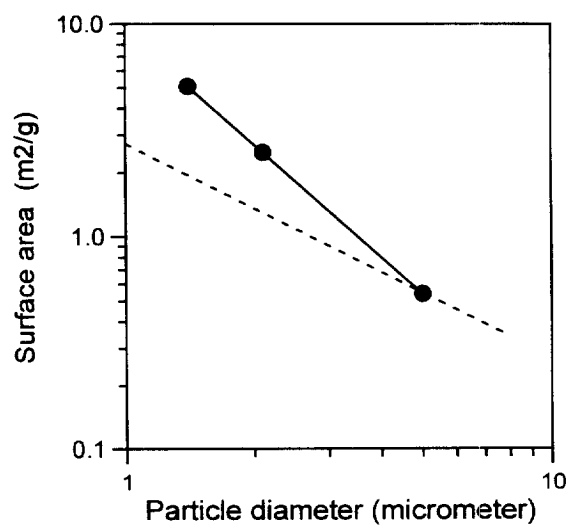

Fig. 2. Comparison of experimental (data points) and theoretical (dashed line) specific surface areas of the prepared non-porous silica.

These theoretically calculated geometrical surface areas are based on a true solid density 2.2 g/ml for the non-porous silica [21]. Those experimental data for 1.4 and 2.1 μm silicas taken from Refs. [24,21], respectively, were determined by using nitrogen as adsorbate and calculated with BET equation, whereas the surface area of the 5 μm silica was determined by a Quantachrome Autosorb 6 [59]. Referring to the theoretical values, the higher experimental surface areas of the silicas having smaller particle diameters indicate that the external surfaces of silicas consist of rugulose.

Silica can be converted into its *n*-alkyl- and phenyl-bonded derivatives with *n*-octadecyl-, *n*-octyl, *n*-butyl, ethyl- and phenyl-dimethylchlorosilanes in the same way [9–11]. The conventional method for chemically bonding with *n*-octadecyldimethylchlorosilane is described briefly in the following [60]. A mixture of *n*-octadecyldimethylchlorosilane and 2,6-lutidine dissolved in dry dichloromethane is added to the silica, which is previously activated in a vacuum furnace. The reaction mixture is stirred and heated under reflux for 24 h. The resultant modified silica is then filtered and thoroughly washed with solvents. The ligand density obtained is ca. 3 μmol/m^2. Since silanol groups at the surface of the silica cannot be reacted completely, the unreacted silanols are normally endcapped by treatment with trimethylchlorosilane. The use of C_{18}-bonded non-porous silica for fast separation of proteins is well demonstrated in the literature. Previous studies suggest that neither column length nor total particle surface area are highly significant factors in the retention of proteins separated by reversed-phase gradient elution chromatography. However, the retention of proteins largely depends on the composition of the mobile phase [5,15]. This implies that the use of non-porous C_{18} silica with a small column is equally effective as conventional packings. With 1.5 μm non-porous silica covalently bound with *n*-octyl functions, the shorter columns provided rapid separation of proteins without loss of resolution [9,11]. When the chain length of bonded akyl-groups was varied, the retention of a set of standard proteins in gradient elution followed the ligand sequence $C_{18}>C_8\approx C_4\approx$phenyl$>C_2$ under constant elution conditions [10].

The non-porous silicas were allowed to react with ether silane and *N*-acetylaminopropyltriethoxysilane to generate bonded phases for hydrophobic interaction chromatography (HIC) of proteins [12]. For the ion-exchange HPLC of proteins, the silica was coated with PEI using a procedure similar to the one introduced by Chang et al. [20] Before incubation with PEI for surface coating, the silica was first modified with γ-glycidoxypropyltrimethoxysilane. The non-porous particles can also be made into a so called tentacle type anion-exchanger by introducing a layer of linear polyelectrolyte chains using a radical grafting polymerization of an *N*-trimethylammoniumethyl-acrylamide salt. Janzen et al. found that the adsorption of BSA on the tentacle-type sorbents fits the Hill equation [19].

In order to prepare the affinity sorbents, silica was surface modified with γ-aminopropyltriethoxysilane, γ-mercaptopropytrimethoxysilane, and γ-glycidoxypyropyltrimethoxysilane, respectively, to obtain the aminopropyl-, mercaptopropyl- and diol-silica. Among these modified silicas, the immobilized ligand (triazine dye) content was highest with the aminopropyl-silica [21]. A stable immunoaffinity sorbent was obtained with the aminopropyl-silica activated by glutaraldehyde and then coupled with protein A. Chromatograms of human IgG on the HPAC column (50×4.6 mm I.D.) packed with immobilized protein A on non-porous silica are shown in Fig. 3. When 9 μl samples of IgG in a concentration ranging from 2.5 to 40 g/l were prepared as the standards, straight lines were obtained from the plots of peak area vs. IgG concentration and also peak height vs. IgG concentration [24]. Experimental data indicated that the column can be used as an analytical column for the determination of IgG contents up to 360 μg in the samples. When pure IgG was applied to the high-performance affinity column, only a minute amount of protein was not retained by the column. The retained proteins could be eluted by stepwise changes from pH 7 to pH 3 as shown in Fig. 3. Changing the pH of the mobile phase is one of the most common and simplest ways to reduce the binding affinity between the protein and the immobilized ligand. A higher value of equilibrium association constant indicates a stronger binding affinity. Usually the association constant and hence the elution time can be reduced significantly by using

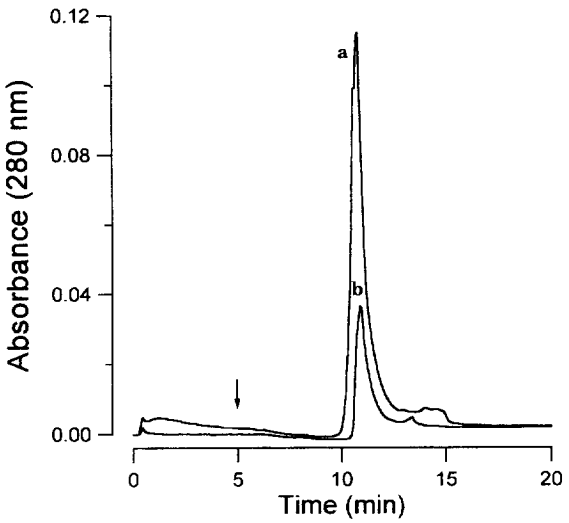

Fig. 3. Chromatography of human IgG on an HPAC column (50×4.6 mm I.D.) packed with immobilized protein A on non-porous silica. The arrows indicate stepwise changes in mobile phase from pH 7 to pH 3. Flow-rate, 1.5 ml/min; sample volume, 9 μl. Sample concentration: $a=30$; $b=10$ g/l [24].

strong elution conditions, e.g., extremely low pH. The strong elution conditions are usually harmful, and therefore fast separation may not be accomplished when retaining the activity of the product and the binding capacity of the column is the most important consideration.

4. Preparation and application of polystyrene-based non-porous sorbents

Many methods have been used to produce non-porous polystyrene-based particles. Maa and Horvath [3] prepared highly crosslinked PS–DVB with a rugulose surface and a mean particle diameter of 3 μm by the method of suspension polymerization. The two-step swelling method developed by Ugelstad et al. [61] was also employed for preparing crosslinked PS–DVB particles having a mean diameter of 2.5 or 2.1 μm [43,47]. In the first step, PS seed emulsion was produced by the emulsifier-free method. In the second step, the size of the particles was increased by swelling with 1-chlorododecane as swelling reagent. After adsorption of monomers, styrene and divinylbenzene, and the initiator, the swollen particles were polymerized at elevated temperature [47]. Based on a similar method, which is called expansion of monodisperse emulsion seed particles, a 4.5 μm, spherical, non-porous PS–DVB (with 10% crosslinking) was produced by Rohm and Hass [40,41].

Non-porous polystyrene with or without crosslinking with DVB can also be prepared by the method of dispersion polymerization. Details of the polymerization procedure were given elsewhere and are summarized in the following [45]. The monomer solution was prepared by mixing styrene with ethanol as the solvent in a flask at 60°C. The initiator (2,2-azobisisobutyronitrile) and stabilizer (polyvinylpyrrolidone) were dissolved in ethanol and mixed with the monomer solution. Polymerization was carried out under nitrogen pressure and stirring at 60°C for 1 day. Non-porous PS beads with a mean diameter of 3.7 μm and a surface area of 1.56 m^2/g was obtained by this recipe. Tuncel et al. used a similar recipe with polyacrylic acid as the stabilizer and a mixture of ethanol and 2-methoxyethanol as the solvent. They obtained monosize PS beads having a diameter of 4 μm [44]. According to Hattori et al. [62], DVB concentrations up to 0.55% (based on total monomer weight) produced stable particles with sizes ranging from 1 to 7 μm using the method of dispersion polymerization with polyvinypyrolidone as the stabilizer. It was found that the particle size of PS was controlled by the amounts of monomer, initiator and stabilizer and the type of dispersion medium, i.e., the solvent, used for polymerization. When the solvent was methanol instead of ethanol, smaller beads having a mean diameter of 2.0 μm could be obtained. Fig. 1 shows the particle size distribution of the 3.7 μm PS beads. The particle size distribution of PS is slightly narrow in compared with that of silica.

To prepare the sorbents for ionic exchange chromatography, the polystyrene-based polymers are derivatized with either PEI coating or latex coating. According to Rounds and Regnier [30], PEI was first adsorbed onto the sulfonated non-porous PS–DVB and then crosslinked by 1,4-butanediol diglycidyl ether. The resulting PEI-coated polystyrene was later methylated to produce a strong anion-exchange packing material. The columns packed with these sorbents were pressure- and pH-stable and allowed

protein separations to be achieved in less than 1 min at ambient temperature. Anion-exchange sorbents can also be made by hydrophobically coating an anion-exchange latex onto unfunctionalized PS–DVB as described by Warth et al. [39] However, the latex-coated resins have not been employed for protein separation.

For use in reversed-phase HPLC, polystyrene beads are alkylated to introduce C_{18} moieties under Friedel–Crafts conditions. Details of the alkylation of non-porous PS–DVB can be found in the literature [47,48]. By using steep gradients with a low dead volume and high flow-rates, the reproducible and quantitative analysis of proteins can be accomplished in less than 1 min on the alkylated non-porous PS–DVB particles having higher chemical and mechanical stability [49].

Only a few studies on the application of non-porous PS in affinity chromatography of proteins have been reported. Tuncel et al. prepared a dye-affinity sorbent by attaching Cibacron Blue F3GA to the poly(vinyl alcohol)-coated PS particles [44]. Before ligand immobilization, poly(vinyl alcohol) was adsorbed on the PS beads and later chemically crosslinked with terephthaldehyde. The main drawback of preparing non-porous sorbents by coating a layer of function groups on the particle surface is that the functional moieties may leak from the sorbents during operation. Wongyai et al. found that crosslinked PS–DVB beads can react with carboxyl-containing compounds such as dinitrophenyl (DNP) amino acids in the presence of carbodiimides as catalyst [43]. This suggested that these beads contain nucleophilic groups on their surface to serve as functional groups for covalent binding of ligands. Affinity chromatography of anti-DNP mouse immunoglobulin E antibody to PS–DVB beads coupled with DNP-lysine was accomplished. In our previous paper [45], a procedure of chemical modification on polystyrene beads was adopted for the derivatization of PS for covalent immobilization of various molecules including low-molecular-mass ligands and proteins. PS was first converted into aromatic amino-containing PS by nitration and successive hydrogenation. In the nitration step, 70% sulfuric acid was present as a catalyst for the production of transient nitronium ion during reaction. The nitration of PS carried out in a mixture of nitric, acetic and sulfuric acids should be concluded within 3 h to avoid any possible sulfonation that could occur. The nitrated PS was converted into aromatic amino-containing PS by hydrogenation in acetic acid with HCl and $SnCl_2$ at 60°C for 2 days. The amino-containing PS is ready for covalently binding of low-molecular-mass ligands using hexamethylene diisocynate as the activator and crosslinker and 1,4-diazo [2,2,2]bicyclooctane (DABCO) as the catalyst for the reactions of amines and isocynates [45]. Protein ligands can also be covalently attached on the amino-containing PS via glutaraldehyde. The utility of the 1 cm column packed with *p*-aminobenzamidine-immobilized non-porous PS for trypsin chromatography is demonstrated in Fig. 4. Elution was achieved by a stepwise change of buffers from Tris–HCl (pH 7.5) to glycine–HCl (pH 2.6). For a sample containing up to 200 μg of trypsin, bound proteins can be eluted completely in ca. 4.5 min following the stepwise change of pH. This suggests that the affinity column was suitable for rapid micropreparative separation even though it is only 1 cm long. A column (50×4.6 mm I.D.) packed with *p*-aminophenyl-β-D-glucopyranoside-immobilized non-porous PS proved to be effective for quantitative analysis of Con A [45]. The immobilization of proteins on the surface of non-porous PS is also accomplished (data are not shown). Columns packed with Con A-immobilized PS are effective for affinity chromatography of Con A-specific proteins and for the determination of intrinsic interaction kinetics between immobilized Con A and its specific sugar.

5. Dynamics of protein adsorption with non-porous particles

5.1. Mathematical model

Modeling work on the prediction of chromatographic performance provides an excellent basis for the design and optimization of a liquid chromatographic process operated either in a preparative or an analytical mode. A large number of papers concerning the simulation of liquid chromatography by the application of numerical methods and computation techniques has been published in recent decades. Early works on simulation of liquid chromatography

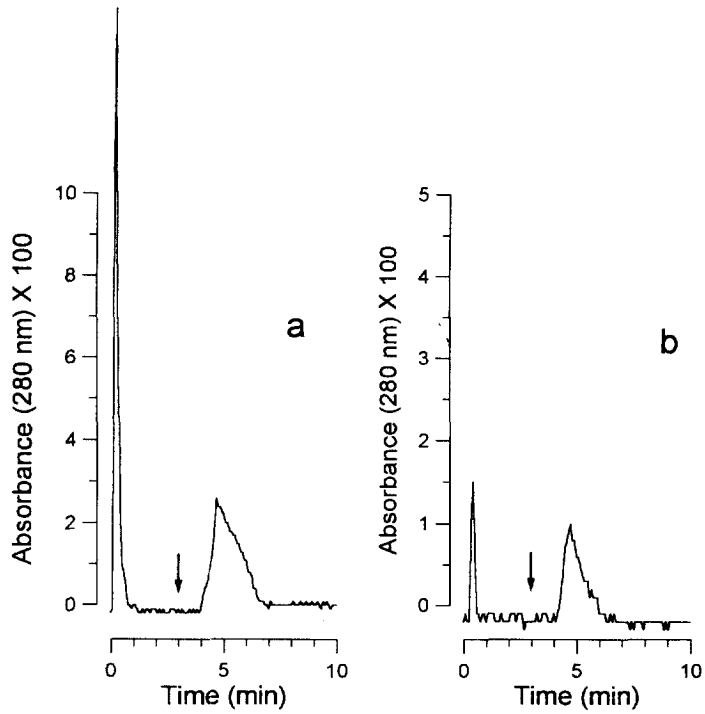

Fig. 4. Chromatography of trypsin on an HPAC column (10×4.6 mm I.D.) packed with *p*-aminobenzamidine-immobilized PS. The arrows indicate stepwise changes in mobile phase from pH 7.5 to 2.6. Flow-rate, 1 ml/min; sample volume, 20 μl. Sample concentration: $a=7.5$; $b=1.0$ g/l [45].

focused on the solution of frontal analysis, whereas the trend of research has shifted to zonal elution under isocratic or gradient conditions in recent years. Among the huge amount of published papers, there have been only a few on the prediction of protein adsorption with non-porous particles in a finite bath and breakthrough curves of a column packed with non-porous sorbents [56,63,64]. The governing equations describing the dynamic adsorption processes of proteins onto non-porous particles in a packed bed can be obtained from the principle of mass conservation as follows:

$$\varepsilon\frac{\partial c}{\partial t}+(1-\varepsilon)\frac{\partial q}{\partial t}+u_0\frac{\partial c}{\partial z}=0 \tag{1}$$

$$\frac{\partial q}{\partial t}=k_a(q_m-q)c-k_d q \tag{2}$$

where c and q are respectively the concentrations of solute in the mobile and the stationary phases. The model consisting of Eqs. (1) and (2) is useful for both affinity and ion-exchange systems, in which the Langmuir adsorption isotherm is properly followed. When both the external film mass transfer and the surface interaction are considered, the forward second-order (adsorption) rate constant k_a and the reversed first-order (desorption) rate constant k_d in Eq. (2) should be regarded as the apparent rate constants. Mao et al. derived the following equation using the equality between the rate of solute transfer from bulk phase to the particle surface and the rate of solute adsorbed on the sorbents [63].

$$\frac{\partial q}{\partial t}=\frac{\frac{6k_f}{d_p}[k_a^{int}(q_m-q)c-k_d^{int}q]}{\frac{6k_f}{d_p}+k_a^{int}(q_m-q)} \tag{3}$$

where k_a^{int} and k_d^{int} are respectively the intrinsic adsorption and desorption rate constants. The equality between Eq. (2) and Eq. (3) is always valid even the rate of adsorption approaches to zero, i.e., at $(\partial q/\partial t)\rightarrow 0$, as a result it holds

$$\frac{k_d}{k_a} = \frac{k_d^{int}}{k_a^{int}} = K_d \quad (4)$$

If the rate of adsorption is other than zero, equating Eqs. (2) and (3) yields

$$\frac{1}{k_a} = \frac{1}{k_a^{int}} + \frac{q_m - q}{\frac{6k_f}{d_p}} \quad (5)$$

Eqs. (4) and (5) describe the relationship between the apparent and the intrinsic rate constants. For a solute concentration varying from zero to the inlet concentration in the liquid (c_0) and the Langmuir isotherm obeyed, a mean value of $q_m - q$ is the average of q_m and $q_m - (q_m K_L c_0)/(1 + K_L c_0)$, i.e.,

$$q_m - q = \frac{q_m}{2}\left(\frac{2 + K_L c_0}{1 + K_L c_0}\right) \quad (6)$$

In this instance, Eq. (5) can be rewritten as

$$\frac{1}{k_a} = \frac{1}{k_a^{int}} + \frac{d_p q_m}{12 k_f}\left(\frac{2 + K_L c_0}{1 + K_L c_0}\right) \quad (7)$$

Eq. (7) is valid for a column with a large sample size, i.e., in frontal analysis, and has also been obtained from other approaches [63,65]. If only an interstitial amount of sample is applied, it is safely assumed that $q_m - q \approx q_m$. Eq. (5) then becomes

$$\frac{1}{k_a} = \frac{1}{k_a^{int}} + \frac{d_p q_m}{6 k_f} \quad (8)$$

Eq. (8) is useful in zonal elution. For a low Reynolds number, as in a common liquid chromatographic process, the mass transfer coefficient, k_f, can be estimated from a J factor correlation proposed by Wilson and Greankoplis [66]. This correlation (Eq. (9)) is valid for liquid with a Reynolds number ($Re = d_p u_0 / v$) range of 0.0016–55 and a Schmidt number ($Sc = v/D_m$) range of 165–70 600

$$J \equiv \frac{k_f}{u_0} Sc^{2/3} = \frac{1.09}{\varepsilon} Re^{-2/3} \quad (9)$$

For the affinity system of IgG-immobilized protein A on 1.4 μm non-porous silica as described elsewhere, k_f was estimated as 3×10^{-2} cm/s at a linear flow velocity of 0.15 cm/s [24]. This k_f value is close to that reported by Mao et al., 3.5×10^{-2} cm/s, for 1.5 μm non-porous particles [63]. With the mass transfer coefficient estimated by Eq. (9), Eqs. (1) and (2), Eqs. (4) and (7) or Eq. (8) can be used as the molding equations for the prediction of the dynamics of protein adsorption in a liquid chromatographic column operated in either frontal or zonal elution mode.

5.2. Predicting the breakthrough curve

Using the definitions of k_a and k_d as described by Eqs. (4) and (7), breakthrough curves can be predicted by solving Eqs. (1) and (2) together with the following initial and boundary conditions.

$$t = 0, c = q = 0 \quad (10a)$$

$$z = 0, c = c_0 \quad (10b)$$

A solution to this model in the case of a step change in input is available in the literature and known as the Thomas solution [67]. The solute concentration profile at the column outlet, i.e., breakthrough curve is [65,68]

$$\frac{c(T, z = L)}{c_0} = \frac{J(nr, nT)}{J(nr, nT) + e^{(1-r)(n-nT)}[1 - J(n, nrT)]} \quad (11)$$

where J is the function defined as

$$J(u, v) = 1 - e^{-v} \int_0^u e^{-\xi} I_0(2\sqrt{v\xi}) d\xi \quad (12)$$

In Eq. (11), the non-dimensional parameters are defined as $r = 1/(1 + K_L c_0)$, $n = (1 - \varepsilon) q_m k_a L / u_0$ and $T = (1 + K_L c_0/(1 - \varepsilon) q_m K_L)$ $(u_0 t / L - \varepsilon)$. The effect of varying the rate constant, particle size, flow-rate and inlet concentration of protein in the liquid on the breakthrough curves has been reported by Mao et al. [63]. However, Eq. (11) indicates that the non-dimensional breakthrough curve is a function of two dimensionless parameters, r and n only. Provided that the rate of adsorption is controlled by the surface interaction, i.e., $(1/k_a^{int} \gg (d_p q_m / 12 k_f)$ $(2 + K_L c_0)/(1 + K_L c_0)$, the non-dimensional rate constant n is not a function of feed concentration. Fig. 5 shows the effects of the non-dimensional adsorption rate constant and the concentration overload on the shape of

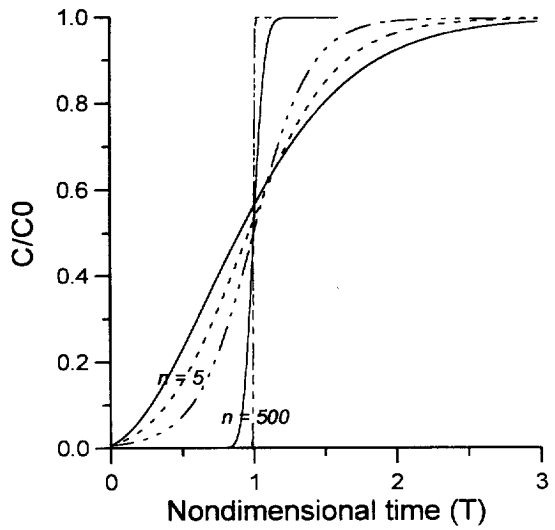

Fig. 5. Dimensional breakthrough curves predicated by Eq. (11) on the effects of non-dimensional parameters n (=5 and 500) and r (——=1, - - - -=0.5, —— - - ——=0).

breakthrough curve. As expected a higher value of the adsorption and mass-transfer rate (higher n value) will lead to a sharper breakthrough curve and hence a more efficient system. When the rate constant is smaller, for example $n=5$, and not adjustable as it is largely determined by the chosen protein–ligand system, the efficiency of the system can only be improved by employing higher feed concentrations that reduce the value of r. In the case of fast adsorption ($n=500$, for example) the breakthrough for $r=0.5$ is not distinguishable from that for $r=0$, as shown in Fig. 5.

Based on this solution, simulation of the adsorption process of proteins in a fixed bed packed with non-porous particles has been carried out by Mao et al. [63]. The determination of thermodynamic and kinetic parameters by means of frontal analysis is conventionally based on the fully breakthrough curve described by Eq. (11). Mao et al. used this model to estimate the appropriate values of the interaction rate constant (k_a^{int}) which would give a satisfactory fit to the experimental curve of a lysozyme–Cibacron Blue F3GA affinity system. During the procedure of curve fitting, they used q_m as the adjustable parameter. However, we found that the binding capacity and the equilibrium association constant can be determined separate from the effect of rate constant. The mean retention time of the breakthrough curve can be derived from Eq. (11) to be [69]

$$t_R = \frac{L}{u_0}\left[\varepsilon + \frac{(1-\varepsilon)q_m K_L}{1+K_L c_0}\right] \tag{13}$$

For estimating parameters K_L and q_m, Eq. (13) can be rewritten as

$$\frac{(1-\varepsilon)L/u_0}{t_R - \varepsilon L/u_0} = \frac{1}{q_m K_L} + \frac{c_0}{q_m} \tag{14}$$

In an actual process the adsorption stage is usually terminated at less than 50% breakthrough. t_{50} denotes the time when the effluent concentration reaches 50% of the inlet concentration. Fig. 6 shows the plots of inlet concentration c_0 with the left hand side (LHS) of Eq. (14). Data points in Fig. 6 indicate the values of the LHS of Eq. (14) with t_R replaced by t_{50} for two typical cases. The agreement between using t_R and t_{50} for the calculation of LHS of Eq. (14) is very good. This suggest that the binding capacity and equilibrium association constant can be

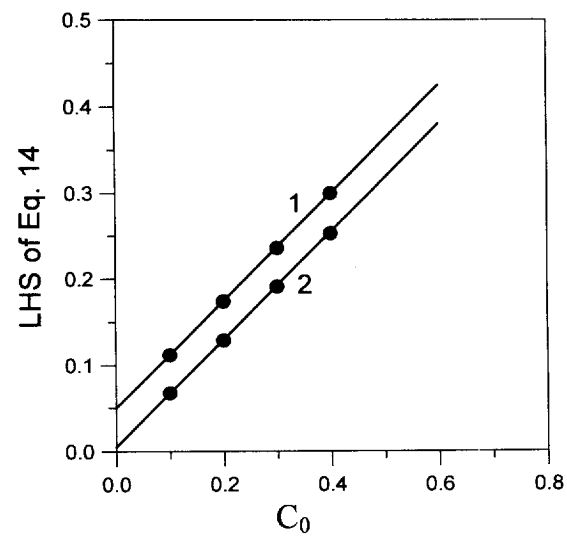

Fig. 6. Plot of the left hand side (LHS) of Eq. (14) vs. feed protein concentration c_0. Solid points indicate the use of t_{50} instead of mean breakthrough time t_R. Parameters used in model simulation for obtaining t_R and t_{50} are: $q_m=5$ g l^{-1}, $k_a=0.6$ l g^{-1} s^{-1} and $K_d=0.0055$ g l^{-1} for curve 1; and $q_m=1.6$ g l^{-1}, $k_a=0.4$ l g^{-1} s^{-1}, $K_d=0.08$ g l^{-1} for curve 2. Other parameters are $d_p=1.5$ μm, flow-rate=0.5 ml/min and $\varepsilon=0.46$. The column dimension is 19×4 mm I.D. from Ref. [63] with permission.

simultaneously determined by running the frontal analysis experiments with varying inlet concentrations and employing t_{50} as the mean retention time.

Upon q_m and K_L being determined, k_a^{int} can be estimated by fitting the experimental breakthrough curves to Eq. (11) with a given k_f value. Experiences in parameter estimation suggest that good fits are limited to the initial part of the breakthrough curves [22,63]. The model always predicted that the column approached saturation faster than that indicated by the experiments. The deviation may be due to a slower non-specific adsorption which follows the specific adsorption at a later time. Mao et al. suggested that heterogeneity of the ligand distribution and the resulting steric hindrance might be the cause of the slow adsorption when the column approaches protein saturation [63]. However, the effect of different adsorption mechanisms, for example the rearrangement of the adsorbed proteins and the multilayer adsorption of proteins on the surface of the modified particles, may also be responsible for this deviation.

In a practical operation of a breakthrough experiment sample application is usually completed at an earlier time of the breakthrough. This time is called the break time, the breakthrough time at which the effluent concentration approaches its maximum permissible level, for example 10% of the inlet concentration. The column capacity that has been used when sample loading is stopped at the break time is called the dynamic binding capacity (DBC), or the effective column capacity [70]. Therefore the DBC is defined as the sample load at which the protein concentration of the effluent is 10% of the input stream. The DBC per unit volume of packed bed is then

$$DBC = (1-\varepsilon)q_m T_b\left(\frac{K_L c_0}{1+K_L c_0}\right) + \varepsilon c_0 \qquad (15)$$

where T_b is the non-dimensional break time which can be derived from Eq. (11) as a function of n and r as shown in Fig. 7. The non-dimension break time increases with n as shown in Fig. 7. For any fixed value of n, the T_b is increased by a decrease in r, that is an increase in sample concentration. In all cases, T_b approaches to unity when n becomes infinite, which means the effects of film mass-transfer and surface interaction resistances are all negligible.

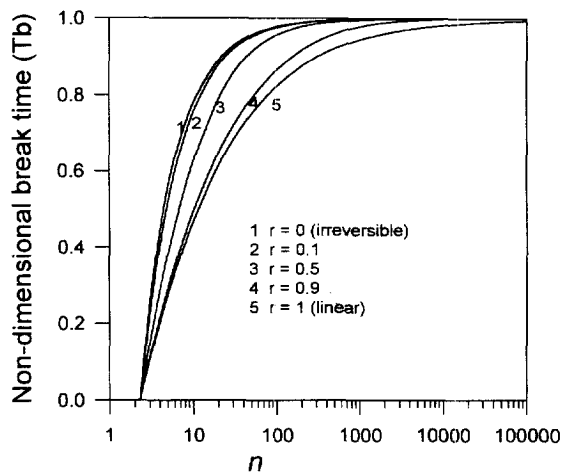

Fig. 7. Non-dimensional break time vs. n with various r.

Obviously, an increase in either c_0, $(1-\varepsilon)q_m$, or T_b increases the DBC. Eq. (15) indicates that the DBC reaches the highest level under the following conditions: (1) low flow-rate, (2) high concentration of solute, (3) large total column binding capacity, and (4) low density of immobilized ligand. Conditions (3) and (4) imply a longer packed bed. Low flow-rate and long packed column both lead to a larger n, and hence a large T_b. Eq. (15) also provides an excellent basis for the determination of binding capacity, equilibrium association constant and adsorption rate constant, as well as for the prediction of the effective column capacity when the column packed with non-porous sorbents is operated for preparative purposes.

5.3. Predicting the performance of pH elution

The chromatogram for application of a small sample to the column, i.e., zonal elution, can also be predicted by the model, Eqs. (1) and (2) with k_a and k_d defined as Eqs. (8) and (4), respectively. The initial and boundary conditions for liquid chromatography with a rectangular input of sample which has a concentration c_0 and an injection interval t_{inj} are

$$t = 0,\ c = q = 0 \qquad (16a)$$

$$z = 0,\ c = \begin{cases} c_0, & 0 \le t \le t_{inj} \\ 0, & \text{otherwise} \end{cases} \qquad (16b)$$

When the column is operated in either the affinity or ion-exchange chromatography mode, the bonded protein can only be eluted by changing the composition of the influent. A stepwise change of the pH of the mobile phase, for example, is the most common method to perform elution of the bound proteins from an affinity column. The rate constants, k_a and k_d, in Eq. (2), in this instance, vary with time during the chromatographic processes. At the adsorption stage ($t<t_e$), these rate parameters are determined under the adsorption conditions. After the elution starting at $t=t_e$, these parameters are determined under the elution conditions. Analytical solutions to Eqs. (1), (2), (16a) and Eq. (16b) are available only when the kinetic rate constants have a constant value, i.e., chromatography in the isocratic elution mode [65,71]. The model simulation by employing a numerical method to simultaneously solve Eqs. (1), (2), (16a), (16b) generates performance information of the elution needed to design an analytical chromatographic process, such as the non-retained fraction, the peak profile and the retention time under various operating conditions. At a limiting case (isocratic elution), the numerical solutions approach the Goldstein solutions [72]. The most important simulated results are summarized in the following.

(1) Effects of the forward rate constant and the equilibrium association constant under adsorption conditions (k_a and K_L) are mainly on the split-peak effect. The non-retained fraction increases with the decrease of k_a and/or the increase of K_L. In addition, the non-retained fraction is also dominated by the sample loading. The split-peak effect becomes more significant when the binding capacity is relatively small compared to the sample load. In a limiting case of irreversible adsorption, simulation of the model yields the non-retained fraction which is in agreement with that estimated by the following expression derived in the literature [73].

$$f=\frac{\ln\left[1+(e^{nQ_i/Q_x}-1)e^{-n}\right]}{nQ_i/Q_x} \tag{17}$$

where Q_i/Q_x is a loading factor, which equals the ratio of the amount of solute injected to the column to the stationary binding capacity of the column.

(2) The rate constant and the equilibrium association constant under both adsorption and elution conditions are responsible for the retention and shape of the elution peak. The influences of these constants under adsorption conditions are inherited from the adsorbate profile along the column length at the beginning of the elution, i.e., the time when the mobile phase changes from the adsorption to the elution stages. In general, slow adsorption kinetics is shown to have a significant dispersive effect on the elution peak. When the rate constant under either adsorption or elution conditions becomes larger, the elution peak becomes sharper and the time required to elute all bound proteins becomes shorter due to the faster rate. The mean retention time of the elution peak is dominated by the equilibrium association constant under elution conditions (K_e). Changing the pH of the mobile phase is the most common way to decrease the K_e value in order to shorten the elution time. The dependence of pH on the variation of K_e is easily obtained experimentally [74,75]. If K_e can not be reduced extensively due to the strong elution conditions which are usually harmful and cause damage to the ligand, a slow ligand density could be considered as an alternative.

(3) In a typical affinity chromatography, the equilibrium association constant under adsorption conditions is extremely large. For the specific interaction between an antibody and an antigen, for example, association constants in the range 10^7–10^8 M^{-1} are generally reported [76]. The adsorption of desired proteins to an immobilized ligand can thus be assumed to be irreversible. When the adsorption is irreversible, the column becomes saturated with the adsorbate from the entrance end. For the chromatographic system near to irreversible adsorption, the simulated elution peaks agree well with those predicted by following equation [24].

$$c(\tau, z=L)=\frac{\sqrt{k_0'/(\tau-1)}}{K_e}\times \frac{I_1[2k_d^*\sqrt{k_0'(\tau-1)}][1-e^{-k_0'k_d^*z_0/L}]}{I_0[2k_d^*\sqrt{k_0'(\tau-1)}]+\Phi[k_d^*(\tau-1),k_0'k_d^*]+e^{-k_0'k_d^*z_0/L}\Phi[k_0'k_d^*,k_d^*(\tau-1)]} \tag{18}$$

where Φ is the function defined as

$$\Phi(u,v)=e^u\int_0^u e^{-s}I_0(2\sqrt{vs})\mathrm{d}s \tag{19}$$

In Eq. (18), K_e ($=k_a/k_d$) is the association constant under the elution conditions and $k_0'=(1-\varepsilon)q_m K_e/\varepsilon$ is the limiting capacity factor, i.e., the capacity factor at zero sample concentration. Fig. 8 shows two simulated elution peaks with different binding capacities and a larger K_L value. However, the $q-z$ profiles at the end of the adsorption stage (Fig. 9) for these systems are not exactly of the rectangular type as those for irreversible adsorption from which Eq. (18) is derived. The approximation of the elution peak by Eq. (18) is valid even in a case in which there is a small amount of non-retained fraction (curve 2 in Fig. 8). Eq. (18) therefore is very useful for determining the values of system parameters and predicating the performance of pH elution.

(4) Either the model simulation or Eq. (18) can predict the effect of sample load on the performance of the elution peak, which provides an excellent basis for choosing a proper plot of peak height vs. sample load as a calibration graph. In general, an increase in adsorption rate constant or a decrease in association constant, either at the adsorption or elution stage, results in an increase in the height of the elution peak. The effect of sample load on the retention time and peak width of the elution peaks is also predictable. The relative sample loading which is represented by the dimensionless group z_0/L in Eq. (18) is the relative length of column saturated with adsorbate before start of elution and equals the loading factor Q_i/Q_x defined in Eq. (17). The model predicts the characteristic decrease of the retention time of the elution peak with increasing overload of sample. When the kinetics of adsorption/desorption are fast the decrease begins at a lower solute loading. This phenomenon is similar to that reported by Wade et al. [71] for the isocratic elution. The feature of peak width increasing with sample load that occasionally appears in experimental reports [32] could also be elucidated by model simulation. The simultaneous reduction of retention time and increase of peak width implies an asymmetry of the elution peaks resulting from an overloaded column.

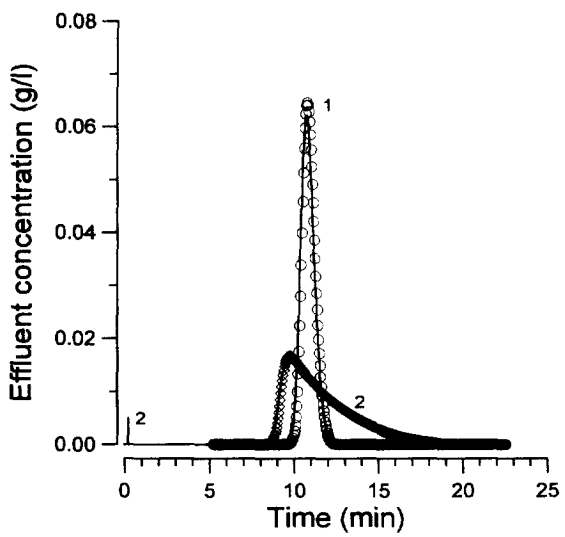

Fig. 8. Comparison of elution profiles from model simulation (solid curves) and the approximated elution profiles (data points) calculated by Eq. (18) for two strong affinity systems. Parameters used for model simulation are: $q_m=35$ g l^{-1}, $K_L=10^8$ M^{-1}, $k_a=0.05$ l g^{-1} s^{-1} (at adsorption stage), $K_e=7.8\times10^4$ M^{-1} ($=0.5$ l g^{-1}) and $k_a=0.7$ l g^{-1} s^{-1} (at elution stage) for curve 1; and $q_m=1$ g l^{-1}, $K_L=10^9$ M^{-1}, $k_a=0.4$ l g^{-1} s^{-1} (at adsorption stage), $K_e=5\times10^6$ M^{-1} and $k_a=5$ l g^{-1} s^{-1} (at elution stage) for curve 2. Other parameters are $\varepsilon=0.39$, $d_p=1.4$ μm, $u_0=0.15$ cm s^{-1}, $L=5$ cm and $c_0=10$ g l^{-1} (in 9 μl sample).

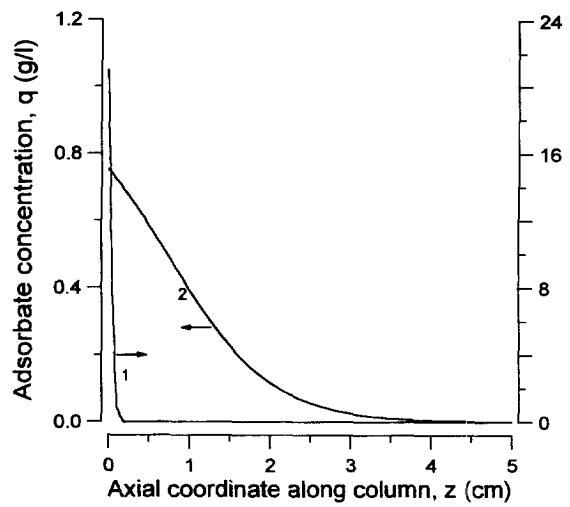

Fig. 9. Distribution of the adsorbate concentration at the starting time of the elution stage as functions of the axial distance along the column for two strong affinity systems as described in Fig. 8.

6. Conclusion and perspective

Non-porous stationary phases based on rigid silica and polymer supports have been well developed for

the separation of proteins since the mid 1980s. Due to the lack of internal porosity, intraparticle diffusion resistances are absent. Rapid separation of slowly diffusing proteins can thus be achieved without loss of their biological activity. The columns packed with non-porous sorbents are usually shorter than the conventional columns since a higher pressure generally arises from use of small particles in order to increase the total surface area for protein binding. Numerous examples in the literature suggest that the columns packed with non-porous sorbents are effective for fast protein separation through the use of higher flow velocities. For use in analytical or micropreparative chromatography of proteins in the reversed-phase, hydrophobic interaction and ion-exchange mode, prepacked columns with non-porous particles having a particle diameter ranging from 2 to 10 μm are commercially available. Preparation of silica- and polystyrene-based affinity sorbents is also possible as discussed in this article. The development of a mathematical model used to describe the dynamics of protein adsorption in liquid chromatographic system is briefly summarized. Those equations provide an excellent basis for the design and optimization of a liquid chromatographic process with non-porous sorbents for either analytical or preparative purposes.

Future developments of non-porous sorbents will include the preparation of non-porous sorbents suitable for HPLC of proteins via the unconventional modes such as hydrophilic interaction, immobilized-metal-ion affinity and mixed-mode interaction. New base materials from synthetic polymers can be made for non-porous sorbents due to the advantage of the ease of preparing various polymers with different chemical compositions on their surface for every particular application. A sophisticated technique for packing the non-porous particles into a narrow column will also be developed. An increased use of HPLC packed with non-porous particles for on-line monitoring of bioprocesses will be seen. Non-porous sorbents offer an important tool for the study on the intrinsic interactions between proteins and immobilized ligands and the molecular basis of protein adsorption mechanisms, for example, the estimation of the intrinsic adsorption rate constant under various conditions of interest and the configurational features of the proteins adsorbed on the immobilized ligands. The experimental data obtained with non-porous sorbents, especially affinity sorbents, will be helpful to study the interaction of a protein to a designed ligand by molecular simulation. To accomplish rapid analysis and fast micropreparative separation, the influences of mobile phase composition and elution strategy coupled with the use of elevated temperatures on the column efficiency should be studied experimentally in cooperation with the model described in this article. Based on the theoretical and experimental studies in the literature, more modeling work will place an emphasis on predicting the performance of gradient elution and displacement chromatography using the non-porous sorbents. Non-porous particles will also be useful for the immobilization of immunological proteins which are usually expensive and available in only very small amounts. The enzyme-linked immunosorbent assays (ELISA) may be executed in a chromatographic format with non-porous particles.

7. List of abbreviations

c	Concentration of solute protein in mobile phase (g l^{-1})
c_o	Sample concentration (g l^{-1})
d_p	Particle diameter of sorbent (cm)
f	Non-retained fraction
k'_0	Capacity factor at zero concentration
k_a	Adsorption rate constant under adsorption or elution conditions (l $g^{-1}s^{-1}$)
k_d	Desorption rate constant under adsorption or elution conditions (s^{-1})
k_f	Film mass-transfer coefficient (cm s^{-1})
k_d^*	Non-dimensional desorption rate constant, defined as $k_d^* = k_d L/u_0$
K_d	Equilibrium dissociation constant (g l^{-1} or M)
K_e	Equilibrium association constant at elution stage (l g^{-1} or M^{-1})
K_L	Equilibrium association constant at adsorption stage (l g^{-1} or M^{-1})
L	Length of the column (cm)
n	Non-dimensional mass-transfer parameter defined as $n = (1-\varepsilon)q_m k_a L/u_0$
q	Sorbate concentration (mass of binding

proteins per unit volume of particle) (g l^{-1})
q_m Maximum sorbate concentration g l^{-1})
Q_i Amount of solute injected to the column (g)
Q_x Saturation binding capacity of the column (g)
r Non-dimensional parameter defined in Eq. (11)
T Non-dimensional time defined in Eq. (11)
T_b Non-dimensional break time
t Time (s)
t_e Time of elution starting (s)
t_{inj} Time interval of sample injection (s)
t_R Retention time of the elution peak or the mean breakthrough time (s)
t_{50} Time of 50% breakthrough (s)
u_0 Superficial velocity (cm s^{-1})
z Linear coordinate along the column (cm)
z_0 Length of the column saturated with adsorbate (cm)

Greek letters
ε Void fraction of the packed column
τ Non-dimensional time defined as $\tau = tu_0/\varepsilon L$
ν dynamic viscosity ($cm^2 s^{-1}$)

Superscripts
int Intrinsic value

Acknowledgments

Support of this work by the National Sience Council of the Republic of China (NSC 84-2214-E194-006) is gratefully acknowledged.

References

[1] H. Chen, Cs. Horvath, J. Chromatogr. A 705 (1995) 32.
[2] Cs. Horvath, B.A. Preiss, S.R. Lipsky, Anal. Chem. 39 (1967) 1422.
[3] Y.-F. Maa, Cs. Horvath, J. Chromatogr. 445 (1988) 71.
[4] Y. Yamasaki, T. Kitamura, S. Nakatani, Y. Kato, J. Chromatogr. 481 (1989) 391.
[5] L.F. Colwell, R.A. Hartwick, J. Liq. Chromatogr. 10 (1987) 2721.
[6] B. de Collongue-Poyet, C. Vidal-Madjar, B. Sebille, K.K. Unger, J. Chromatogr. A 664 (1995) 155.
[7] L. Varady, L.K. Kalghatgi, Cs. Horvath, J. Chromatogr. 458 (1988) 207.
[8] F.B. Anspach, A. Johnston, H.-J. Wirth, K.K. Unger, M.T.W. Hearn, J. Chromatogr. 499 (1990) 103.
[9] K.K. Unger, G. Jilge, J.N. Kinkel, M.T.W. Hearn, J. Chromatogr. 359 (1986) 61.
[10] G. Jilge, R. Janzen, H. Giesche, K.K. Unger, J.N. Kinkel, M.T.W. Hearn, J. Chromatogr. 397 (1987) 71.
[11] R. Janzen, K.K. Unger, H. Giesche, J.N. Kinkel, M.T.W. Hearn, J. Chromatogr. 397 (1987) 81.
[12] R. Janzen, K.K. Unger, H. Giesche, J.N. Kinkel, M.T.W. Hearn, J. Chromatogr. 397 (1987) 91.
[13] K. Kalghatgi, Cs. Horvaath, J. Chromatogr. 398 (1987) 335.
[14] K. Kalghatgi, Cs. Horvath, J. Chromatogr. 443 (1988) 343.
[15] N. Nimura, H. Itoh, T. Kinoshita, N. Nagae, M. Nomura, J. Chromatogr. 585 (1991) 207.
[16] H. Itoh, N. Nimura, T. Kinoshita, N. Nagae, M. Nomura, Anal. Biochem. 199 (1991) 7.
[17] D.O. O'Keefe, A.M. Paiva, Anal. Biochem. 230 (1995) 48.
[18] A. Rudolphi, K.-S. Boos, D. Seidel, Chromatographia 41 (1995) 645.
[19] R. Janzen, K.K. Unger, W. Muller, M.T. Hearn, J. Chromatogr. 522 (1990) 77.
[20] S.H. Chang, K.M. Gooding, F.E. Regnier, J. Chromatogr. 120 (1976) 321.
[21] B. Anspach, K.K. Unger, J. Davies, M.T.W. Hearn, J. Chromatogr. 457 (1988) 195.
[22] A.I. Liapis, B. Anspach, M.E. Findley, J. Davies, M.T.W. Hearn, K.K. Unger, Biotechnol. Bioeng. 34 (1989) 467.
[23] H.J. Wirth, K.K. Unger, M.T.W. Hearn, J. Chromatogr. 550 (1990) 383.
[24] W.-C. Lee, C.-Y. Chuang, J. Chromatogr. A 721 (1996) 31.
[25] G.K. Bonn, K. Kalghatgi, W.C. Horne, Cs. Horvath, Chromatographia 30 (1990) 484.
[26] D.J. Burke, J.K. Duncan, L.C. Dunn, L. Cummings, C.J. Siebert, G.S. Ott, J. Chromatogr. 353 (1986) 425.
[27] D.J. Burke, J.K. Duncan, C. Siebert, G.S. Ott, J. Chromatogr. 359 (1986) 533.
[28] J.K. Duncan, A.J.C. Chen, C.J. Siebert, J. Chromatogr. 397 (1987) 3.
[29] I. Mazsaroff, M.A. Rounds, F.E. Regnier, J. Chromatogr. 411 (1987) 452.
[30] M.A. Rounds, F.E. Regnier, J. Chromatogr. 443 (1988) 73.
[31] T. Hashimoto, J. Chromatogr. 544 (1991) 257.
[32] Y. Kato, T. Kitamura, A. Mitsi, T. Hashimoto, J. Chromatogr. 398 (1987) 327.
[33] D.B. DeWald, J.R. Colca, J.M. McDonald, J.D. Pearson, J. Liq. Chromatogr. 11 (1988) 2109.
[34] S. Nakatani, T. Kitamura, Y. Yamasaki, Y. Kato, Chromatographia 31 (1991) 505.
[35] Y. Kato, T. Kitamura, S. Nakatani, T. Hashimoto, J. Chromatogr. 483 (1989) 401.
[36] F.D. Antia, I. Fellegvari, Cs. Horvath, Ind. Eng. Chem. Res. 34 (1995) 2796.

[37] Y. Kato, S. Nakatani, T. Kitamura, Y. Yamasaki, T. Hashimoto, J. Chromatogr. 502 (1990) 416.
[38] E. Watson, F. Yao, J. Chromatogr. 594 (1992) 392.
[39] L.M. Warth, J.S. Fritz, J.O. Naples, J. Chromatogr. 462 (1989) 165.
[40] R.F. Strasburg, J.S. Fritz, J.O. Naples, J. Cromatogr. 547 (1991) 11.
[41] Y. Miura, J.S. Fritz, J. Chromatogr. 482 (1989) 155.
[42] J.M. Varga, S. Wongyai, P. Fritsch, G. Bonn, Chromatographia 30 (1990) 527.
[43] S. Wongyai, J.M. Varga, G.K. Bonn, J. Chromatogr. 536 (1991) 155.
[44] A. Tuncel, A. Denizli, D. Purvis, C.R. Lowe, E. Piskin, J. Chromatogr. 634 (1993) 161.
[45] W.-C. Lee, C.-H. Lin, R.-C. Ruaan, K.-Y. Hsu, J. Chromatogr. A 704 (1995) 307.
[46] C.G. Huber, P.J. Oefner, E. Preuss, G.K. Bonn, Nucleic Acids Res. 21 (1993) 1061.
[47] C.G. Huber, P.J. Oefner, G.K. Bonn, Anal. Biochem. 212 (1993) 351.
[48] C.G. Huber, P.J. Oefner, G.K. Bonn, Anal. Chem. 67 (1995) 578.
[49] C.G. Huber, P.J. Oefner, G.K. Bonn, Chromatographia 37 (1993) 653.
[50] G. Pastores, C. Lonardo, B. Variano, M.L. Anderson, J. Liq. Chromatogr. 18 (1995) 3049.
[51] S. Hjerten, J.-L. Liao, J. Chromatogr. 457 (1988) 165.
[52] S. Hjerten, J. Mohammad, K.-O. Eriksson, J.-L. Liao, Chromatographia. 31 (1991) 85.
[53] J.-L. Liao, S. Hjerten, J. Chromatogr. 457 (1988) 175.
[54] J. Mohammad, K.-O. Eriksson, G. Johansson, J. Biochem. Biophys. Methods 26 (1993) 41.
[55] J.-P. Li, S. Hjerten, J. Biochem. Biophys. Methods 22 (1991) 311.
[56] M.A. McCoy, B.J. Hearn, A.I. Liapis, Chem. Eng. Comm. 108 (1991) 225.
[57] J. Yu, Z. El Rassi, J. Chromatogr. 646 (1993) 143.
[58] W. Stober, A. Fink, E. Bohn, J. Colloid Interface Sci. 26 (1968) 62.
[59] Y. Nishikawa, Anal. Sci. 7 (1991) 637.
[60] J.N. Kinkel, K.K. Unger, J. Chromatogr. 316 (1984) 193.
[61] J. Ugelstad, P.C. Mork, K. Herder Kaggerud, T. Ellingsen, A. Berge, Adv. Colloid Interface Sci. 13 (1980) 101.
[62] M. Hattori, E.D. Sudol, M.S. El-Aasser, J. Appl. Polym. Sci. 50 (1993) 2027.
[63] Q.M. Mao, A. Johnston, I.G. Prince, M.T.W. Hearn, J. Chromatogr. 548 (1991) 147.
[64] Q.M. Mao, R. Stockmann, I.G. Prince, M.T.W. Hearn, J. Chromatogr. 646 (1993) 67.
[65] F.H. Arnold, H.W. Blach, J. Chromatogr. 355 (1986) 13.
[66] E.J. Wilson, C.J. Greankoplis, Ind. Eng. Chem. Fundam. 5 (1966) 9.
[67] H.C. Thomas, J. Am. Chem. Soc. 66 (1994) 1664.
[68] N.K. Hiester, T. Vermeulen, Chem. Eng. Prog. 48 (1952) 505.
[69] W.-C. Lee, G.J. Tsai, G.T. Tsao, J. Chromatogr. 504 (1990) 55.
[70] A.M. Tsai, D. Englert, E.E. Graham, J. Chromatogr. 504 (1990) 55.
[71] J.L. Wade, A.F. Bergold, P.W. Carr, Anal. Chem. 59 (1987) 1286.
[72] S. Goldstein, Proc. R. Soc. London A 219 (1953) 151.
[73] A. Jaulmes, C. Vidal-Madjar, Anal. Chem. 63 (1991) 1165.
[74] K.P. Antonsen, C.K. Colton, M.L. Yarmush, Biotechnol. Prog. 7 (1991) 159.
[75] K.A. Kang, D.D. Ryu, Biotechnol. Prog. 7 (1991) 205.
[76] M.L. Yarmush, A.H. Weiss, K.P. Antosen, D.J. Odde, D.M. Yarmush, Biotechnol. Adv. 10 (1992) 413.